Electronic Journal of Biotechnology 27 (2017) 84–90

Contents lists available at ScienceDirect

Electronic Journal of Biotechnology

Research article

Immobilization of horseradish peroxidase on Fe_3O_4 magnetic nanoparticles

Saleh A. Mohamed [a,b,*], Majed H. Al-Harbi [a], Yaaser Q. Almulaiky [a], Ibrahim H. Ibrahim [a], Reda M. El-Shishtawy [c,d]

[a] Biochemistry Department, Faculty of Science, King Abdulaziz University, Jeddah, Saudi Arabia
[b] Molecular Biology Department, National Research Center, Dokki, Cairo, Egypt
[c] Chemistry Department, Faculty of Science, King Abdulaziz University, Jeddah, Saudi Arabia
[d] Dyeing, Printing and Textile Auxiliaries Department, Textile Research Division, National Research Center, Dokki, Cairo, Egypt

ARTICLE INFO

Article history:
Received 29 November 2016
Accepted 30 March 2017
Available online 4 April 2017

Keywords:
Activity
Energy dispersive X-ray
FT-IR spectroscopy
Immobilized enzymes
Immobilized
Iron
Magnetic separation
pH
Protein immobilization
Scanning electron microscopy
Soluble horseradish peroxidase

ABSTRACT

Background: Iron magnetic nanoparticles have attracted much attention. They have been used in enzyme immobilization because of their properties such as product is easily separated from the medium by magnetic separation. The present work was designed to immobilize horseradish peroxidase on Fe_3O_4 magnetic nanopraticles without modification.
Results: In the present study, horseradish peroxidase (HRP) was immobilized on non-modified Fe_3O_4 magnetic nanoparticles. The immobilized HRP was characterized by FT-IR spectroscopy, scanning electron microscopy, and energy dispersive X-ray. In addition, it retained 55% of its initial activity after 10 reuses. The optimal pH shifted from 7.0 for soluble HRP to 7.5 for the immobilized HRP, and the optimal temperature shifted from 40°C to 50°C. The immobilized HRP is more thermostable than soluble HRP. Various substrates were oxidized by the immobilized HRP with higher efficiencies than by soluble HRP. K_m values of the soluble and immobilized HRP were 31 and 45 mM for guaiacol and 5.0 and 7.0 mM for H_2O_2, respectively. The effect of metals on soluble and immobilized HRP was studied. Moreover, the immobilized HRP was more stable against high concentrations of urea, Triton X-100, and isopropanol.
Conclusions: Physical immobilization of HRP on iron magnetic nanoparticles improved the stability toward the denaturation induced by pH, heat, metal ions, urea, detergent, and water-miscible organic solvent.

1. Introduction

Immobilized enzymes have several advantages over soluble enzymes such as retention and repeating of their catalytic activities. The stabilization of enzyme activity was the most important character for immobilizing enzymes. The immobilized enzymes were useful in diagnostics, bioaffinity chromatography, and biosensor applications. Compared with macromaterials as immobilization matrix, nanomaterials are characterized by high surface area, low mass transfer limitation, and high mobility of particles [1]. Immobilization of enzyme on nanomaterials avoids several problems such as enzyme leaching [2], enzyme 3D structure loss [3], and strong diffusion resistance. The surface area of nanomaterials would be expected to provide better adsorption of enzyme. Enzyme loadings with nanomaterials were also found to be higher than that of macro-scale supporting materials, probably owing to their large surface area [4].

In the past few decades, iron magnetic nanoparticles have attracted much attention. Magnetic metal nanoparticles have been used in protein/enzyme immobilization because of their unique properties such as superparamagnetism, large surface area, large surface-to-volume ratio, and easy separation under external magnetic fields [5,6]. Fe_3O_4 magnetic nanoparticles are the most prevalent materials because they have low toxicity and good biocompatibility [7,8]. Because bare iron magnetic nanoparticles often have high reactivity and easily undergo degradation upon direct exposure to certain environments, leading to poor stability and dispersity [9,10], various modification methods have been developed to utilize soluble and biocompatible iron magnetic nanoparticles for protein immobilization [11]. Several polymers such as polyethylene glycol, polyvinylpyrrolidone, poly(ethylene-co-vinyl acetate), poly(lactic-co-glycolic acid), polyvinyl alcohol, and acrylic polymer have also been used as coating materials in aqueous

* Corresponding author.
E-mail address: saleh38@hotmail.com (S.A. Mohamed).
Peer review under responsibility of Pontificia Universidad Católica de Valparaíso.

http://dx.doi.org/10.1016/j.ejbt.2017.03.010

suspension [12,13]. Moreover, natural dispersants including gelatin, dextran, polylactic acids, starch, albumin, liposomes, chitosan, and ethyl cellulose have been extensively used for coating in aqueous medium [14,15,16,17].

Because immobilized enzymes can be reused several times during applications, one has to avoid the laborious work of filtration of the product; however, this process is accompanied by some inevitable loss of the matrix, and this can be avoided by selecting magnetic nanoparticles as the matrix so that the product is easily separated from the medium by magnetic separation. Considering this information, the present work was designed to immobilize HRP on Fe_3O_4 magnetic nanoparticles without modification.

2. Materials and methods

2.1. Horseradish peroxidase and magnetic nanoparticles (Fe_3O_4)

Horseradish peroxidase (HRP) was previously purified from horseradish cv. Balady. The detailed process was reported in our previous paper [18]. Fe_3O_4 was purchased from Sigma-Aldrich and used as received.

2.2. Peroxidase assay

Peroxidase activity was determined according to Yuan and Jiang [19]. The reaction mixture contained in 1 mL, 8 mM H_2O_2, 40 mM guaiacol, 50 mM sodium acetate buffer, pH 5.5, and the least amount of enzyme preparation. The change of absorbance at 470 nm due to guaiacol oxidation was recorded at 30-s intervals. One unit of peroxidase activity is defined as the amount of enzyme that increases the OD by 1.0 per min under standard assay conditions.

2.3. Immobilization procedure

Enzyme immobilization was performed by end-over-end on Fe_3O_4 magnetic nanoparticles with HRP dissolved in 50 mM sodium acetate buffer pH 4.0 or Tris–HCl buffer pH 7.0 or 8.0 at room temperature overnight. Aliquots of the supernatant were drawn, and the magnetic nanoparticles were dried at room temperature to verify the progress of immobilization. The immobilization efficiency % was calculated from the following formula:

$$\text{Immobilization efficiency } \% = \text{Activity of immobilized enzyme/Initial activity of soluble enzyme} \times 100$$

2.4. Structure characterization

The FTIR spectra of samples were obtained on a PerkinElmer spectrum 100 FT-IR spectrometer. The morphology of the samples scanning electron microscopy (SEM) and its energy dispersive X-ray (EDX) were characterized by field emission scanning electron microscopy (JEOL JSM-7600F, Japan). The microscope was operated at an acceleration voltage of 2 kV and 10 mm work distance carbon film.

2.5. Reuse of immobilized enzymes

The reusability of the immobilized enzyme was studied by repeated usage for approximately 10 times. The activity determined the first time was considered 100% for the calculation of remaining percentage activity after each use.

2.6. Physicochemical characterization of the enzyme

Kinetic studies were performed using different concentrations of guaiacol and H_2O_2 as substrates. The K_m was calculated from the Lineweaver–Burk double reciprocal plots. The optimal temperature and pH for soluble and immobilized HRP were determined by incubating the enzyme in pH ranging from 4.0 to 9.0 and temperature ranging from 30°C to 80°C. The thermal stability was determined by incubating the enzyme at different temperatures for 15 min. The enzyme was taken out and kept in ice bath for 5 min. Then H_2O_2 and guaiacol were added for the determination of the enzyme activity. The highest activity was taken as 100%.

2.7. Effect of metal ions

The effects of various metal ions on the enzyme activity of soluble and immobilized HRP were determined by pre-incubating the enzyme with 2 and 5 mM metal ions for 15 min before adding H_2O_2 and guaiacol. The activity in the absence of the metal ions was taken as 100%.

2.8. Effect of urea, organic solvents, and Triton X-100

The enzyme activity of soluble and immobilized HRP was determined by assaying the enzyme in the presence of urea, Triton X-100, or isopropanol. The enzyme activity without exposure to these compounds was considered 100%.

3. Results and discussion

Physical immobilization can be considered the simplest functionalization method employed in protein immobilization as it may be easily performed by just dipping the material into a solution containing the target biomolecules, and no additional coupling reagents, surface treatment, and protein modification are required [20, 21,22]. A number of physically immobilized proteins based on iron magnetic nanoparticles have been developed. For example, glucose oxidase was immobilized onto Fe_3O_4 magnetic nanoparticles by a physical method for water deoxygenation, and 78% immobilization was obtained, with a specific activity of 640 U/g [23]. In the present study, HRP was immobilized on non-modified Fe_3O_4 magnetic nanoparticles. Immobilization efficiency is affected by the concentration of nanoparticles, concentration of HRP in solution, and pH of the solution, which were optimized in this study. Fig. 1a shows the dependence of the immobilization efficiency of HRP on Fe_3O_4 magnetic nanoparticles concentration. Immobilization efficiency was enhanced with increase in Fe_3O_4 concentration up to approximately 200 mg and then decreased. Fig. 1b shows that the immobilization efficiency of HRP increases with increasing initial concentrations of HRP up to 188 units. The effect of pH on immobilization efficiency was studied (Fig. 1c). The maximum immobilization efficiency of HRP was detected at pH 8.0.

It has been reported that metals oxides can form stable monolayers by binding with ligands as long as their isoelectric points are lower than the pKa of ligands [24]. Because the isoelectric point of Fe_3O_4 is 6.5–6.8 [25], which is lower than the pKa of HRP (above 8 [26]), it is expected that a slightly alkaline pH around 8 would favor HRP immobilization onto Fe_3O_4 through its carboxyl groups.

The ATR-FTIR spectra of the magnetite nanoparticles Fe_3O_4 and Fe_3O_4-HRP samples are shown in Fig. 2. Both samples exhibit similar absorption peaks with observed differences. Before HRP immobilization onto Fe_3O_4, characteristic absorption peaks centered at 557 cm^{-1} are due to the Fe-O vibrations of Fe_3O_4 [27]. In addition, adsorbed water molecules onto the surface of Fe_3O_4 are manifested by their bending modes of vibration at 1653 cm^{-1} and the O—H stretching vibrations that centered at 3393 cm^{-1} [27]. After HRP immobilization onto Fe_3O_4, a large and broad band is observed at 3333 cm^{-1}, indicating the presence of both the OH and NH_2 groups of water and HRP molecules, respectively. The peak formed by the bending modes of water molecules observed in the case of the Fe_3O_4 sample has become enlarged and shifted after HRP immobilization. Because HRP is a polypeptide and a biopolymer, its amide I and II would be observed in

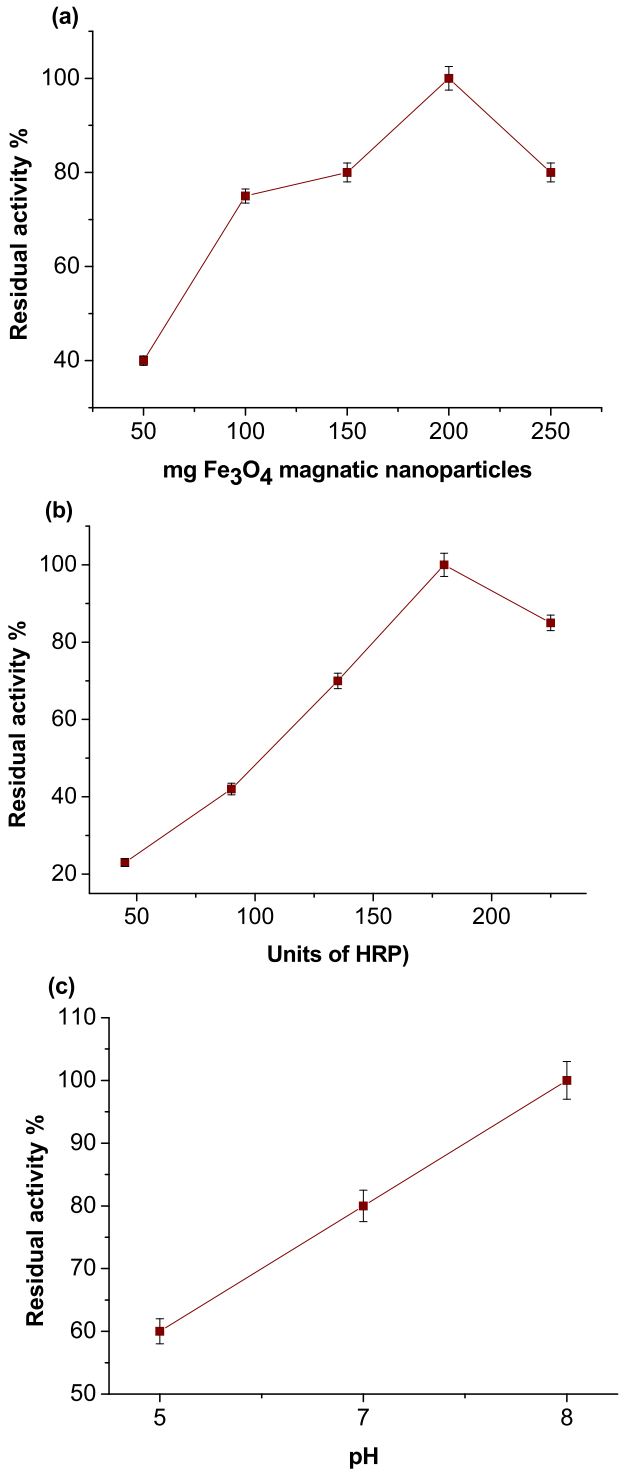

Fig. 1. Effect of Fe_3O_4 magnetic nanoparticle concentration (a), initial HRP concentration (b), and pH (c) on the immobilization efficiency of HRP. Each point represents the average of three experiments ± S.E.

the FTIR spectra [28,29,30]. The Fe_3O_4-HRP sample in Fig. 2 shows the appearance of amide I stretching peak due to C═O and amide II bending peak due to N—H around 1636 and 1541 cm^{-1}, respectively. Moreover, C—O stretching peak is clearly observed in Fe_3O_4-HRP sample, indicating the success of HRP immobilization onto Fe_3O_4.

The SEM images of Fe_3O_4 and Fe_3O_4-HRP samples are shown in Fig. 3. The SEM images show a typical agglomeration of magnetic nanoparticles with a better surface coverage and the appearance of

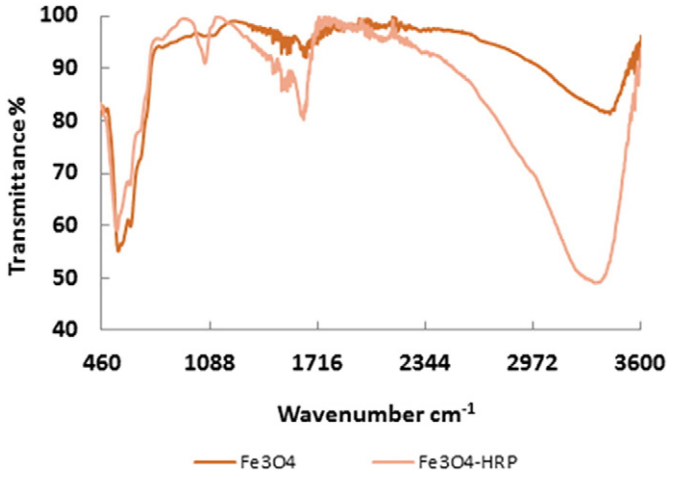

Fig. 2. FT-IR spectra of Fe_3O_4 magnetic nanoparticle and Fe_3O_4-HRP.

large particles in the case of Fe_3O_4-HRP samples compared with those of Fe_3O_4. The EDX patterns of Fe_3O_4 and Fe_3O_4-HRP are shown in Fig. 4, and their elemental compositions are summarized in Table 1. Carbon peaks appear because of the use of carbon tapes during EDX measurement. It is clearly observed that the percentage of elemental composition has changed upon HRP immobilization onto Fe_3O_4, and a simple calculation based on both carbon and oxygen content would indicate a rough percentage in the range of 6.6–10.8% of HRP immobilization. We previously studied the vibrating sample magnetometer (VSM) behavior of Fe_3O_4 before and after mixing with other materials, and the results indicated similar behavior of hysteresis but with lower saturation magnetization in accordance with its content in the mixture [31]. Because EDX data (Table 1) confirmed that 7% of the HRP was immobilized, it was expected that the saturation magnetization will be slightly affected accordingly.

The reusability of the immobilized enzyme was detected after enzyme assay and washing the support with water to remove the substrate and products and regain enzyme assay. As shown in Fig. 5, the HRP immobilized on magnetic nanoparticles retained 55% of its initial activity after 10 reuses, indicating that the immobilized HRP has appropriate stability and can be reused. After the fifth repeated use, β-cyclodextrin-capped silver nanoparticle-HRP (AgNP-HRP) retained 97% of its original activity [32].

The effect of pH on the activity of soluble and immobilized HRP was evaluated by incubating these preparations in buffers of varying pH values ranging from 4.0 to 9.0 (Fig. 6a). The pH shifted from 7.0 for soluble HRP to 7.5 for the HRP immobilized on magnetic nanoparticles, which retained significantly higher enzyme activity both in acidic and alkaline pH compared to the soluble enzyme. AgNP-HRP preparation showed no change in pH optimum (pH 8.0) [32]. Lee et al. [33] reported that the activity of soluble HRP is maximal near pH 7.0, and HRP immobilized on multi-wall carbon nanotubes exhibits its activity over a broad range of pH values between 4 and 9. On the contrary, HRP immobilized on gold nanoparticles showed the same pH optimum as their soluble counterpart, i.e., pH 5.0 [34].

The optimal temperature of soluble HRP shifted from 40°C to 50°C for HRP immobilized on magnetic nanoparticles (Fig. 6b). The thermal stability of soluble and immobilized HRP was also studied (Fig. 6c). The results showed that the immobilized HRP is more thermostable than soluble HRP at all temperature tested from 40°C to 80°C. Ni et al. [34] showed that both HRP immobilized on gold nanoparticles and free HRP had good activity performance during long-time incubation at 25°C. Moreover, the immobilized HRP had much higher activity than the free form at 50°C, which indicated that the immobilized HRP had better thermostability than free HRP. The thermal stability of HRP

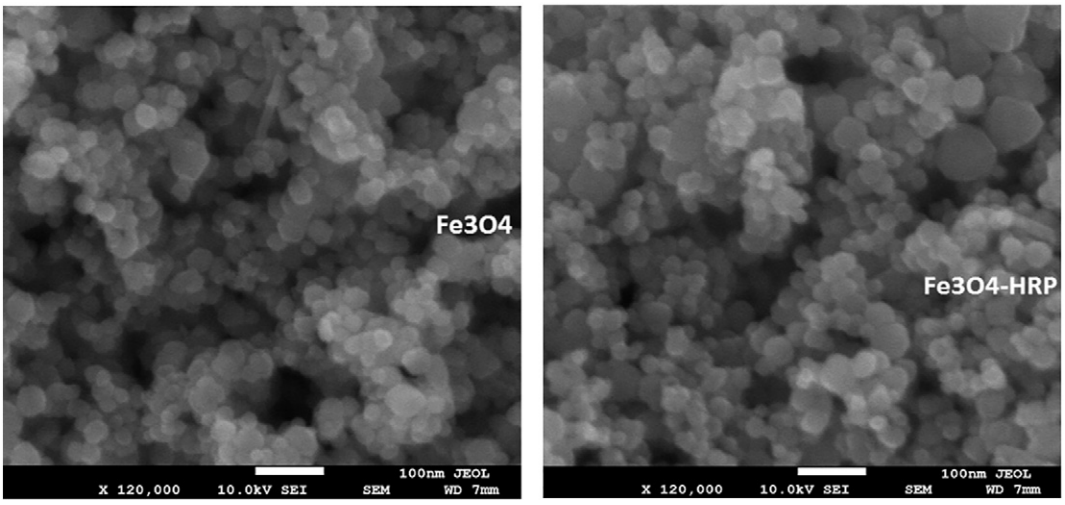

Fig. 3. SEM images of Fe_3O_4 magnetic nanoparticle and Fe_3O_4-HRP.

immobilized on nanoporous silica, SBA-15 is significantly improved in comparison with free HRP [35].

Table 2 shows the substrate specificity of soluble HRP and HRP immobilized on magnetic nanoparticles. Various substrates were oxidized by immobilized HRP with higher efficiencies than those of soluble HRP. The enzyme activity on guaiacol was considered 100% activity. Oxidation activity was in the order *o*-phenylenediamine > *o*-dianisidine > *p*-aminoantipyrine > pyrogallo > ABTS with 69%, 29%, 22%, 12%, and 4% relative activity of soluble HRP, respectively. However, oxidation activity was in the order *o*-phenylenediamine > *p*-aminoantipyrine > *o*-dianisidine > pyrogallo > ABTS with 100%, 90%, 60%, 28%, and 25% relative activity of Immobilized HRP, respectively. Valerio et al. [36] reported that reduction in the affinity of the immobilized enzyme for the substrate compared to the soluble form could be attributed to the high concentration of protein that was immobilized, generating diffusion effects, and the change of active site of enzyme after contact with the solid surface of the support. Fig. 7 shows that the K_m values of the soluble HRP and HRP immobilized on magnetic nanoparticles were 31 and 45 mM for guaiacol and 5.0 and 7.0 mM for H_2O_2, respectively. The results showed that the soluble HRP had more affinity toward guaiacol and H_2O_2 than the immobilized HRP. In the same manner, K_m of H_2O_2 and K_m of 3′, 3′, 5′, 5′-tetramethylbenzidine by HRP immobilized on gold nanoparticles increased from 0.91 and 0.19 to 1.90 and 0.42 mM, respectively, indicating the reduced affinity of HRP to both the substrates [34].

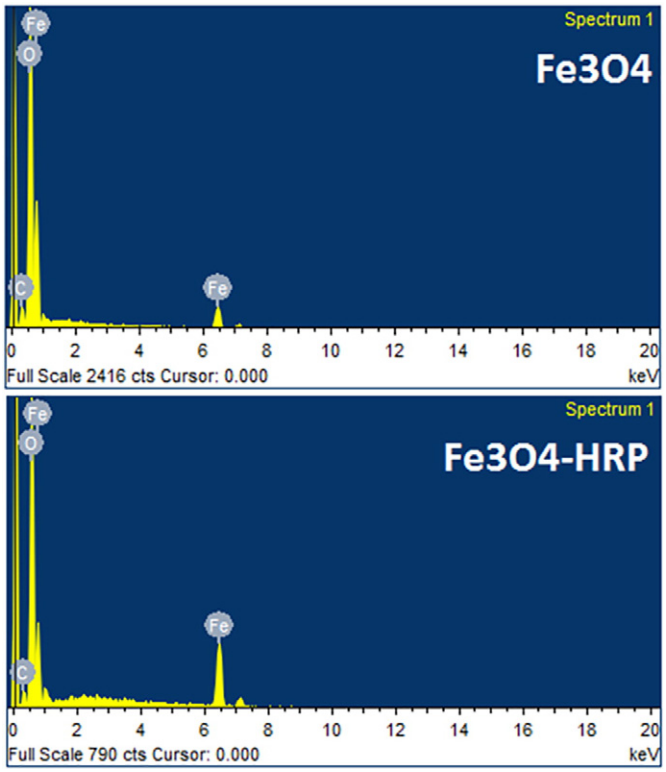

Fig. 4. SEM–EDX spectra of Fe_3O_4 magnetic nanoparticle and Fe_3O_4-HRP.

Table 1
Elemental composition of Fe_3O_4 magnetic nanoparticle and Fe_3O_4-HRP.

	Fe_3O_4		Fe_3O_4-HRP	
Elements	Weight%	Atomic%	Weight%	Atomic%
Carbon	3.20 ± 0.05	8.14 ± 0.14	3.74 ± 0.15	8.68 ± 0.25
Oxygen	28.67 ± 0.35	54.66 ± 1.5	34.75 ± 1.5	60.59 ± 2.3
Iron	68.12 ± 1.2	37.20 ± 1.0	61.51 ± 2.0	30.72 ± 0.95

Each value represents the mean of three experiments ± S.E.

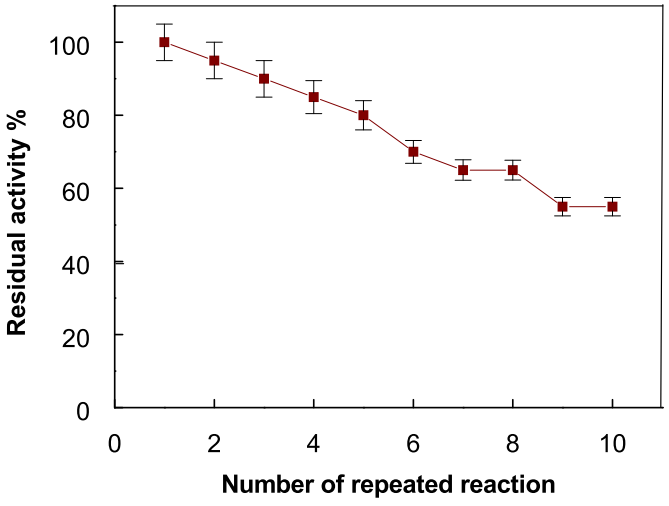

Fig. 5. Reuse of HRP immobilized on Fe_3O_4 magnetic nanoparticle. Each point represents the mean of three experiments ± S.E.

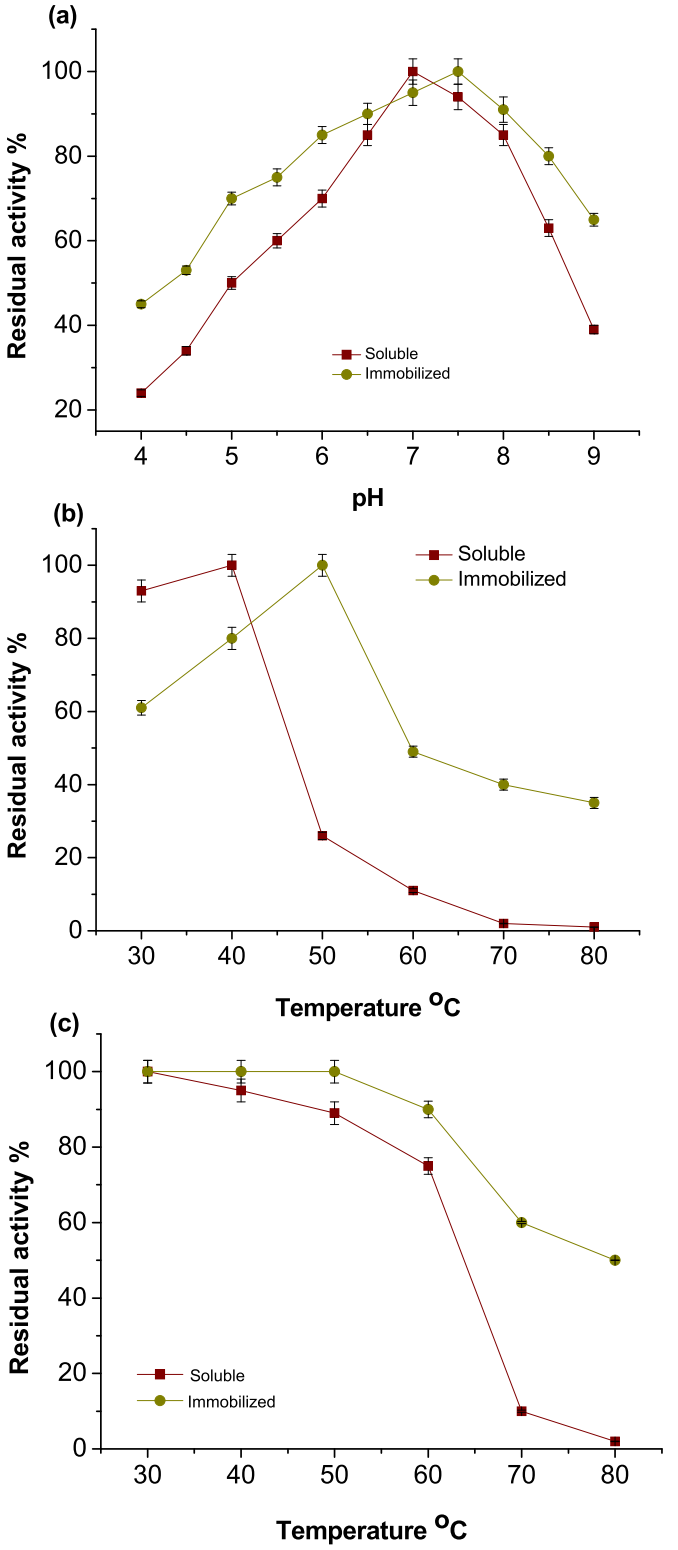

Fig. 6. Optimum pH (a), optimum temperature (b), and thermostability (c) of soluble HRP and HRP immobilized on Fe_3O_4 magnetic nanoparticle. Each point represents the average of three experiments ± S.E.

The effect of metals on soluble HRP and HRP immobilized on magnetic nanoparticles was studied (Table 3). Fe^{2+} had strong activation for immobilized HRP compared to soluble HRP. Cu^{2+} also caused an activation effect for immobilized HRP and had no effect on soluble HRP. All metals tested had less inhibitory effect on immobilized HRP than on soluble HRP except for Hg^{2+}, which caused a strong inhibitory effect on soluble HRP. Zn^{2+} completely inhibited the soluble HRP activity. The results detected that HRP immobilized on magnetic nanoparticles had higher resistance toward metal ions at 2 mM and 5 mM than the soluble enzyme. Several studies have reported that proteins may unfold upon contact with urea because of its direct interaction with the peptide backbone through hydrogen

Table 2
Substrate specificity of soluble HRP and HRP immobilized on Fe_3O_4 magnetic nanoparticle. The activity with the guaiacol was considered 100%.

	Relative activity %	
Substrate	Soluble HRP	Immobilized HRP
o-Phenylenediamine	69 ± 1.95	100 ± 2.2
o-Dianisidine	29 ± 0.75	90 ± 2.7
p-Aminoantipyrine	22 ± 0.56	60 ± 1.9
Pyrogallol	12 ± 0.25	28 ± 0.65
ABTS	4 ± 0.10	25 ± 0.75

ABTS: 2,2′-azino-bis(3-ethylbenzothiazoline-6-sulphonic acid).
Each value represents the mean of three experiments ± S.E.

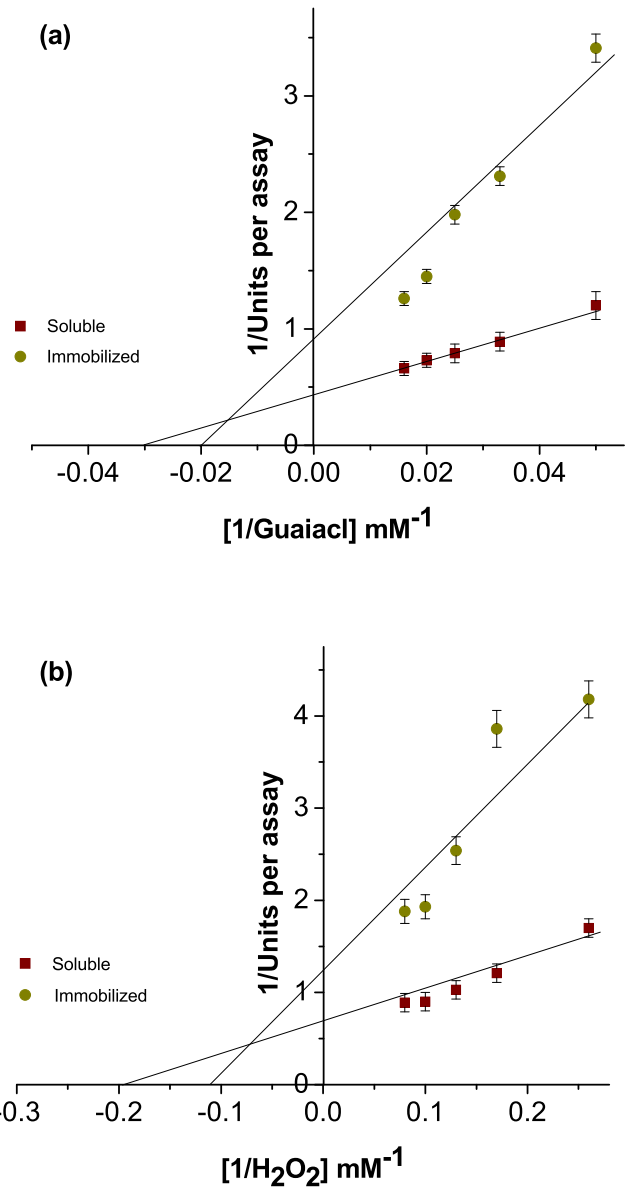

Fig. 7. Lineweaver–Burk plot relating soluble HRP and HRP immobilized on Fe_3O_4 magnetic nanoparticle reaction velocity to guaiacol (a) and H_2O_2 (b) concentrations. Each point represents the average of three experiments ± S.E.

Table 3
Effect of metal ions on soluble HRP and HRP immobilized on Fe_3O_4 magnetic nanoparticle.

	Relative activity%			
	Soluble HRP		Immobilized HRP	
Metal ion	2 mM	5 mM	2 mM	5 mM
Control	100 ± 2.90	100 ± 1.86	100 ± 3.15	100 ± 2.80
Cu^{2+}	100 ± 3.10	92 ± 2.21	150 ± 3.45	130 ± 1.65
Co^{2+}	70 ± 1.10	71 ± 1.95	88 ± 3.12	80 ± 2.11
Cd^{2+}	78 ± 1.50	30 ± 1.20	91 ± 2.35	85 ± 2.41
Ni^{2+}	72 ± 1.88	62 ± 1.67	78 ± 1.55	70 ± 2.11
Zn^{2+}	0.0	0.0	56 ± 1.08	29 ± 0.95
Hg^{2+}	45 ± 1.65	30 ± 0.75	75 ± 1.85	63 ± 1.66
Pb^{2+}	54 ± 1.29	45 ± 1.25	70 ± 2.14	62 ± 1.85
Fe^{2+}	159 ± 3.65	96 ± 2.65	280 ± 4.77	168 ± 3.11

Each value represents the mean of three experiments ± S.E.

bonds and/or hydrophobic interactions, which contribute to the maintenance of protein conformation [37,38]. Nanoparticle-bound HRP was more resistant to inactivation induced by urea compared to its soluble counterpart. The effect of concentration of urea on the activity of the soluble HRP and HRP immobilized on magnetic nanoparticles was studied (Table 4). The immobilized HRP retained 60% and 33% of its activity at 2 and 4 M urea, respectively, while soluble enzyme retained 44% and 12%, respectively. Similarly, the exposure of soluble HRP to 4 M urea for 2 h resulted in a loss of 70% activity, although AgNP-HRP retained more than 80% of the initial enzyme activity [32]. HRP immobilized on SBA-15 pores exhibited significant improvement of resistance to urea exposure compared with the free enzyme, with only ~20% denaturation at 5 M urea, where the free enzyme activity dropped to 10%. The bound enzyme activity dropped to 16% only at 10 M urea [35].

The activity of the soluble HRP and HRP immobilized on magnetic nanoparticles was tested in the presence of Triton X-100 (Table 4). The immobilized HRP exhibited 88% and 77% activity at 5% and 10% Triton X-100, whereas the soluble enzyme showed 56% and 11% activity, respectively. The results indicated that the immobilized HRP was markedly more resistant to Triton X-100 than the soluble HRP. The activity of the soluble HRP and HRP immobilized on magnetic nanoparticles was monitored in the presence of isopropanol (Table 4). Isopropanol caused a slight inhibition effect on the activity for immobilized HRP compared to that on soluble HRP.

4. Conclusion

Although enzymes physically immobilized on iron magnetic nanoparticles is simple and mild, this method generally involves comparatively weak interactions such as electrostatic interactions [39,40], hydrogen bonds [41], van der Waals forces [42,43,44], and hydrophobic interactions [44], and the binding stability of the adsorbed species is highly affected by environmental conditions (pH, temperature, ionic strength, and biomolecule concentration). On the contrary, our results appeared that the physical immobilization of HRP on iron magnetic nanoparticles improved their stability toward the denaturation induced by pH, heat, metal ions, urea, detergent, and water–miscible organic solvent. The immobilization of HRP on iron magnetic nanoparticles appeared promising in several practical applications.

Table 4
Effect of chemical compounds on soluble HRP and HRP immobilized on Fe_3O_4 magnetic nanoparticle.

		Relative activity%	
Chemical	Concentration	Soluble HRP	Immobilized HRP
Control	–	100 ± 2.75	100 ± 1.85
Urea	2 M	44 ± 1.15	60 ± 1.88
	4 M	12 ± 0.35	33 ± 0.75
Triton X-100	5%	56 ± 1.25	88 ± 2.23
	10%	11 ± 0.23	77 ± 1.26
Isopropanol	5%	42 ± 0.85	90 ± 1.78
	10%	35 ± 0.66	75 ± 1.45

Each value represents the mean of three experiments ± S.E.

Conflict of interest

The authors declare that they have no conflict of interest.

References

[1] Wang P. Nanoscale biocatalyst systems. Curr Opin Biotechnol 2006;17:574–9. http://dx.doi.org/10.1016/j.copbio.2006.10.009.

[2] Manyar HG, Gianotti E, Sakamoto Y, Terasaki O, Coluccia S, Tumbiolo S. Active biocatalysts based on pepsin immobilized in mesoporous SBA-15. J Phys Chem C 2008;112:18110–6.

[3] Hong J, Gong P, Xu D, Dong L, Yao S. Stabilization of α-chymotrypsin by covalent immobilization on amine-functionalized superparamagnetic nanogel. J Biotechnol 2007;128:597–605. http://dx.doi.org/10.1016/j.jbiotec.2006.11.016.

[4] Liu W, Wang L, Jiang R. Specific enzyme immobilization approaches and their application with nanomaterials. Top Catal 2012;55:1146–56. http://dx.doi.org/10.1007/s11244-012-9893-0.

[5] Xu P, Zeng GM, Huang DL, Feng CL, Hu S, Zhao MH, et al. Use of iron oxide nanomaterials in wastewater treatment: A review. Sci Total Environ 2012;424:1–10. http://dx.doi.org/10.1016/j.scitotenv.2012.02.023.

[6] Tang WW, Zeng GM, Gong JL, Liang J, Xu P, Zhang C, et al. Impact of humic/fulvic acid on removal of heavy metals from aqueous solutions using nanomaterials affected by humic/fulvic acid: A review. Sci Total Environ 2014;468-469:1014–27. http://dx.doi.org/10.1016/j.scitotenv.2013.09.044.

[7] Liu Y, Jia S, Wu Q, Ran J, Zhang W, Wu S. Studies of Fe_3O_4-chitosan nanoparticles prepared by co-precipitation under the magnetic field for lipase immobilization. Catal Commun 2011;12:717–20. http://dx.doi.org/10.1016/j.catcom.2010.12.032.

[8] Gao J, Gu H, Xu B. Multifunctional magnetic nanoparticles: Design, synthesis, and biomedical applications. Acc Chem Res 2009;42:1097–107. http://dx.doi.org/10.1021/ar9000026.

[9] Zhao GX, Wen T, Yang X, Yang SB, Liao JL, Hu J, et al. Preconcentration of U(VI) ions on few-layered graphene oxide nanosheets from aqueous solutions. Dalton Trans 2012;41:6182–8. http://dx.doi.org/10.1039/C2DT00054G.

[10] Zong PF, Wang SF, Zhao YL, Wang H, Pan H, He CH. Synthesis and application of magnetic graphene/iron oxides composite for the removal of U(VI) from aqueous solutions. Chem Eng J 2013;220:45–52. http://dx.doi.org/10.1016/j.cej.2013.01.038.

[11] Reddy LH, Arias JL, Nicolas J, Couvreur P. Magnetic nanoparticles: Design and characterization, toxicity and biocompatibility, pharmaceutical and biomedical applications. Chem Rev 2012;112:5818–78. http://dx.doi.org/10.1021/cr300068p.

[12] Lee H, Lee E, Kim DK, Jang NK, Jeong YY, Jon S. Antibiofouling polymer-coated superparamagnetic iron oxide nanoparticles as potential magnetic resonance contrast agents for *in vivo* cancer imaging. J Am Chem Soc 2006;128:7383–9. http://dx.doi.org/10.1021/ja061529k.

[13] Mohamed SA, Al-Ghamdia SS, El-Shishtawy RM. Immobilization of horseradish peroxidase on amidoximated acrylic polymer activated by cyanuric chloride. Int J Biol Macromol 2016;91:663–70. http://dx.doi.org/10.1016/j.ijbiomac.2016.06.002.

[14] Souza KC, Ardisson JD, Sousa EMB. Study of mesoporous silica/magnetite systems in drug controlled release. J Mater Sci Mater Med 2009;20:507–12. http://dx.doi.org/10.1007/s10856-008-3592-1.

[15] Sun C, Veiseh O, Gunn J, Fang C, Hansen S, Lee D, et al. *In vivo* MRI detection of gliomas by chlorotoxin-conjugated superparamagnetic nanoprobes. Small 2008;4:372–9. http://dx.doi.org/10.1002/smll.200700784.

[16] Mahmoudi M, Simchi A, Imani M, Milani AS, Stroeve P. *In vivo* MRI detection of gliomas by chlorotoxin-conjugated superparamagnetic nanoprobes. J Phys Chem B 2008;112:14470–81. http://dx.doi.org/10.1021/jp803016n.

[17] Liu HL, Ko SP, Wu JH, Jung MH, Min JH, Lee JH, et al. One-pot polyol synthesis of monosize PVP-coated sub-5 nm Fe_3O_4 nanoparticles for biomedical applications. J Magn Magn Mater 2007;310:815–7. http://dx.doi.org/10.1016/j.jmmm.2006.10.776.

[18] Mohamed SA, Abulnaja KO, Ads AS, Khan JA, Kumosani TA. Characterization of an anionic peroxidase from horseradish cv. Balady Food Chem 2011;128:725–30. http://dx.doi.org/10.1016/j.foodchem.2011.03.096.

[19] Yuan ZY, Jiang TJ. Horseradish peroxidase. In: Whitaker JR, Voragen A, Wong DWS, editors. Handbook of food enzymology. New York: Marcel Dekker Inc.; 2003. p. 403–11.

[20] Ozturk N, Akgol S, Arisoy M, Denizli A. Reversible adsorption of lipase on novel hydrophobic nanospheres. Sep Purif Technol 2007;58:83–90. http://dx.doi.org/10.1016/j.seppur.2007.07.037.

[21] Valdes-Solis T, Rebolledo AF, Sevilla M, Valle-Vigon P, Bomati-Miguel O, Fuertes AB, et al. Preparation, characterization, and enzyme immobilization capacities of superparamagnetic silica/iron oxide nanocomposites with mesostructured porosity. Chem Mater 2009;21:1806–14. http://dx.doi.org/10.1021/cm8005937.

[22] Betancor L, Luckarift HR. Bioinspired enzyme encapsulation for biocatalysis. Trends Biotechnol 2008;26:566–72. http://dx.doi.org/10.1016/j.tibtech.2008.06.009.

[23] Mahdizadeh F, Karimi A, Ranjbarian L. Immobilization of glucose oxidase on synthesized superparamagnetic Fe_3O_4 nanoparticles; application for water deoxygenation. Int J Sci Eng Res 2012;3:516–20.

[24] Folkers JP, Gorman CB, Laibinis PE, Buchholz S, Whitesides GM. Self-assembled monolayers of long-chain hydroxamic acids on the native oxides of metals. Langmuir 1995;11:813–24. http://dx.doi.org/10.1021/la00003a024.
[25] Kosmulski M. Chemical properties of material surfaces. Marcel Dekker; 2001.
[26] Hashimoto S, Takeuchi H. Protonation and hydrogen-bonding state of the distal histidine in the CO complex of horseradish peroxidase as studied by ultraviolet resonance Raman spectroscopy. Biochemistry 2006;45:9660–7. http://dx.doi.org/10.1021/bi060466f.
[27] Kumari M, Pittman CU, Mohan D. Heavy metals [chromium (VI) and lead (II)] removal from water using mesoporous magnetite (Fe_3O_4) nanospheres. J Colloid Interface Sci 2015;442:120–32. http://dx.doi.org/10.1016/j.jcis.2014.09.012.
[28] Mohamed SA, Al-Malki AL, Kumosani TA, El-Shishtawy RM. Horseradish peroxidase and chitosan: Activation, immobilization and comparative results. Int J Biol Macromol 2013;60:295–300. http://dx.doi.org/10.1016/j.ijbiomac.2013.06.003.
[29] Surewicz WK, Mantsch HH. New insight into protein secondary structure from resolution-enhanced infrared spectra. Biochim Biophys Acta 1988;952:115–30. http://dx.doi.org/10.1016/0167-4838(88)90107-0.
[30] Kaposi AD, Fidy J, Manas ES, Vanderkooi JM, Wright WW. Horseradish peroxidase monitored by infrared spectroscopy: Effect of temperature, substrate and calcium. Biochim Biophys Acta 1999;1435:41–50. http://dx.doi.org/10.1016/S0167-4838(99)00206-X.
[31] Salam MA, El-Shishtawy RM, Obaid AY. Synthesis of magnetic multi-walled carbon nanotubes/magnetite/chitin magnetic nanocomposite for the removal of Rose Bengal from real and model solution. J Ind Eng Chem 2014;20:3559–67. http://dx.doi.org/10.1016/j.jiec.2013.12.049.
[32] Karim Z, Khan MJ, Maskat MY, Adnan R. Immobilization of horseradish peroxidase on β-cyclodextrin capped silver nanoparticles: Its future aspects in biosensor application. Prep Biochem Biotechnol 2015;46:321–7. http://dx.doi.org/10.1080/10826068.2015.1031389.
[33] Lee Y-M, Kwon O-Y, Yoon Y-J, Ryu K. Immobilization of horseradish peroxidase on multi-wall carbon nanotubes and its electrochemical properties. Biotechnol Lett 2006;28:39–43. http://dx.doi.org/10.1007/s10529-005-9685-8.
[34] Ni Y, Li J, Huang Z, He K, Zhuang J, Yang W. Improved activity of immobilized horseradish peroxidase on gold nanoparticles in the presence of bovine serum albumin. J Nanopart Res 2013;15:2038. http://dx.doi.org/10.1007/s11051-013-2038-y.
[35] Ikemoto H, Chi Q, Ulstrup J. Stability and catalytic kinetics of horseradish peroxidase confined in nanoporous SBA-15. J Phys Chem C 2010;114:16174–80. http://dx.doi.org/10.1021/jp103137e.
[36] Valerio SG, Alves JS, Klein MP, Rodrigues RC, Hertz PF. High operational stability of invertase from *Saccharomyces cerevisiae* immobilized on chitosan nanoparticles. Carbohydr Polym 2013;92:462–8. http://dx.doi.org/10.1016/j.carbpol.2012.09.001.
[37] Ashraf H, Husain Q. Stabilization of DEAE cellulose adsorbed and glutaraldehyde crosslinked white radish (*Raphanus sativus*) peroxidase. J Sci Ind Res 2010;69:613–20.
[38] Tanford C. Theoretical models for the mechanism of denaturation. Adv Protein Chem 1970;24:1–95.
[39] Guisan JM. Immobilization of enzymes and cells. 2nd ed. Madrid, Spain: Humana Press Inc.; 2006.
[40] Liang Y-Y, Zhang L-M, Li W, Chen R-F. Polysaccharide-modified iron oxide nanoparticles as an effective magnetic affinity adsorbent for bovine serum albumin. Colloid Polym Sci 2007;285:1193–9. http://dx.doi.org/10.1007/s00396-007-1672-2.
[41] Joshi MD, Sidhu G, Pot I, Brayer GD, Withers SG, McIntosh LP. Hydrogen bonding and catalysis: A novel explanation for how a single amino acid substitution can change the pH optimum of a glycosidase. J Mol Biol 2000;299:255–79. http://dx.doi.org/10.1006/jmbi.2000.3722.
[42] Zhang Y, Li J, Han D, Zhang H, Liu P, Li C. An efficient resolution of racemic secondary alcohols on magnetically separable biocatalyst. Biochem Biophys Res Commun 2008;365:609–13. http://dx.doi.org/10.1016/j.bbrc.2007.10.205.
[43] Vijayalakshmi A, Tarunashree Y, Baruwati B, Manorama SV, Narayana BL, Johnson REC, et al. Enzyme field effect transistor (ENFET) for estimation of triglycerides using magnetic nanoparticles. Biosens Bioelectron 2008;23:1708–14. http://dx.doi.org/10.1016/j.bios.2008.02.003.
[44] Chen J-P, Lin W-S. Sol-gel powders and supported sol-gel polymers for immobilization of lipase in ester synthesis. Enzyme Microb Technol 2003;32:801–11. http://dx.doi.org/10.1016/S0141-0229(03)00052-8.